Check for updates

Bifunctional earth-abundant phosphate/phosphide catalysts prepared *via* atomic layer deposition for electrocatalytic water splitting†

Jan Rongé, [‡a] Thomas Dobbelaere, [‡b] Lowie Henderick, [b] Matthias M. Minjauw, [b] Sreeprasanth Pulinthanathu Sree, [a] Jolien Dendooven, [b] Johan A. Martens [a] and Christophe Detavernier*[b]

The development of active and stable earth-abundant catalysts for hydrogen and oxygen evolution is one of the requirements for successful production of solar fuels. Atomic Layer Deposition (ALD) is a proven technique for conformal coating of structured (photo)electrode surfaces with such electrocatalyst materials. Here, we show that ALD can be used for the deposition of iron and cobalt phosphate electrocatalysts. A PE-ALD process was developed to obtain cobalt phosphate films without the need for a phosphidation step. The cobalt phosphate material acts as a bifunctional catalyst, able to also perform hydrogen evolution after either a thermal or electrochemical reduction step.

Introduction

Producing hydrogen by splitting water using solar energy is one of the most attractive routes towards the production of renewable fuels. Solar water splitting devices operate at low current density as determined by the photon flux from the sun, which allows for less stringent device requirements. Due to the large catalytic surface area, earth-abundant catalyst materials are required to avoid issues of scarcity and cost. Cobalt phosphate is a well-known earth-abundant oxygen evolution reaction (OER) catalyst that self-assembles from cobalt and phosphate ions at neutral pH.[1] Its structure is that of a cobalt oxyhydroxide with incorporated phosphate ions that act as proton acceptors during water oxidation.[2] Cobalt-based catalysts can be operated in acidic and basic solutions as well.[3,4] Bloor *et al.* achieved overall water splitting in acidic media containing phosphate and cobalt ions.[4] By applying a cell potential in excess of 2 V, phosphate containing cobalt catalysts were deposited on the anode and cathode and performed oxygen evolution and hydrogen evolution, respectively. The hydrogen evolution reaction (HER) catalyst consisted of a metallic cobalt core and a surface layer containing cobalt, phosphorus and oxygen, similar to the bifunctional cobalt phosphate catalyst reported by Cobo *et al.*[5] Cobalt phosphide (CoP) is known to be among the most active and stable earth-abundant HER catalysts.[6,7] Related phases such as Co_2P and even amorphous Co–P material were found to be active towards HER as well.[8] The amorphous material was deposited by electrodeposition and could be purified by a potential cycling procedure to reach a Co : P stoichiometric ratio of 1 : 1.[9] Consequently, several authors have demonstrated bifunctional cobalt-based phosphate/phosphide catalysts.[5,10,11] Jiang *et al.* electrodeposited Co–P films with very low phosphorus content yet excellent HER and OER activity.[10] A similar evolution occurred for iron phosphide (FeP), which is a bifunctional catalyst as well and even outperforms CoP as a HER catalyst, although it is less stable.[12,13] However, the reports on overall water splitting using iron phosphide catalysts are rare.[11,14] Interestingly, Kibsgaard *et al.* predicted a near-zero hydrogen adsorption free energy on ternary $Fe_{0.5}Co_{0.5}P$ and demonstrated that consequentially this material has superior performance to both monometallic phases.[15]

Metal phosphides are commonly synthesized *via* phosphidation of metallic or oxide nanoparticles,[6,12,13] electrodeposition,[3,5,10,11] or solid-state reactions using precursor salts.[8,14,15] Chemical vapor deposition may also be used.[8] However, for the envisioned water splitting applications, a synthesis strategy is often required that is able to precisely coat surfaces. Atomic layer deposition (ALD) has been used to deposit protective coatings, passivation layers and transparent catalytic films.[16,17] Yang *et al.* have deposited cobalt oxide films on silicon photoanodes to simultaneously protect the electrode from corrosion and catalyse the OER.[18] Goryachev *et al.* obtained cobalt phosphide films by phosphidation of cobalt oxide, deposited by ALD.[19] Di Palma *et al.* have recently reported ALD deposited cobalt phosphate films which were used for OER.[20]

[a]*Centre for Surface Chemistry and Catalysis, KU Leuven, Celestijnenlaan 200F, 3001 Leuven, Belgium*

[b]*Department of Solid State Sciences, Ghent University, Krijgslaan 281 S1, 9000 Gent, Belgium. E-mail: Christophe.Detavernier@UGent.be*

† Electronic supplementary information (ESI) available. See DOI: 10.1039/c9na00391f

‡ Equal contributions.

A number of ALD processes for iron phosphate have been developed by different authors, mostly with the goal of using the material as a lithium-ion battery electrode.[21–23] Some of the authors have developed a plasma-enhanced (PE-ALD) method which has the advantage of having much higher growth per cycle (GPC) values than other processes, speeding up deposition times for thicker films.[22,24] In this work, ALD was used to deposit cobalt and iron phosphate films with electrocatalytic activity for both HER and OER. In addition, post-deposition thermal reduction was used to obtain phosphide electrocatalysts for HER. Contrary to previous reports which started from metal phosphides, phosphates were used as the starting material in this work. A PE-ALD process has been developed using the same phosphate source as the reported iron phosphate process[22] but combined with $Co(Cp)_2$ as the cobalt precursor. This precursor had been previously used for the PE-ALD growth of Co_3O_4 by Donders et al.[25]

Results & discussion

Deposition

We start this section with a brief characterization of the PE-ALD deposition process for cobalt phosphate. The process characterization was performed by running 50-cycle test depositions within a range of substrate temperatures (at constant pulse durations) and with varying pulse durations (at a constant substrate temperature) on silicon substrates. In situ spectroscopic ellipsometry measurements were acquired after each cycle and fitted with a generalized oscillator model, allowing calculation of the film thickness after each cycle.

The results are summarized in Fig. 1. Fig. 1a shows in situ growth curves acquired at substrate temperatures ranging from 150 to 325 °C, using a fixed pulse sequence of 10 s TMP plasma – 20 s O_2 plasma – 7 s $CoCp_2$ vapor. The slope of the growth curve (i.e. the GPC) decreases with increasing temperature, as shown explicitly in Fig. 1b. Above 275 °C, there is a distinct nonlinearity between 10 and 30 cycles, which is attributed to nucleation effects; therefore, the GPC was calculated from the linear region which appeared after 35 cycles. The increasing GPC at low temperatures is attributed to a CVD contribution originating from TMP plasma polymerization, an effect that has been previously investigated in detail.[22] To avoid this and to ensure a PE-ALD growth mode, a substrate temperature of 300 °C is chosen for all further depositions. The influence of the pulse duration on the GPC at this temperature is shown in Fig. 1c–e for respectively the TMP plasma, O_2 plasma, and $CoCp_2$ vapor exposures. For each curve, one exposure time was varied, while the two others were fixed to the circled values (10 s, 20 s, and 7 s for respectively TMP plasma, O_2 plasma, and $CoCp_2$ vapor). While the TMP plasma and $CoCp_2$ vapor exposures show relatively quick saturation, the O_2 plasma pulse saturates rather slowly. Note that the process also works without O_2 plasma (the 0 s point, i.e. a TMP plasma – $CoCp_2$ process), albeit at a much lower GPC of approx. 0.1 nm per cycle compared to the saturated value of 0.8 nm per cycle for the full process.
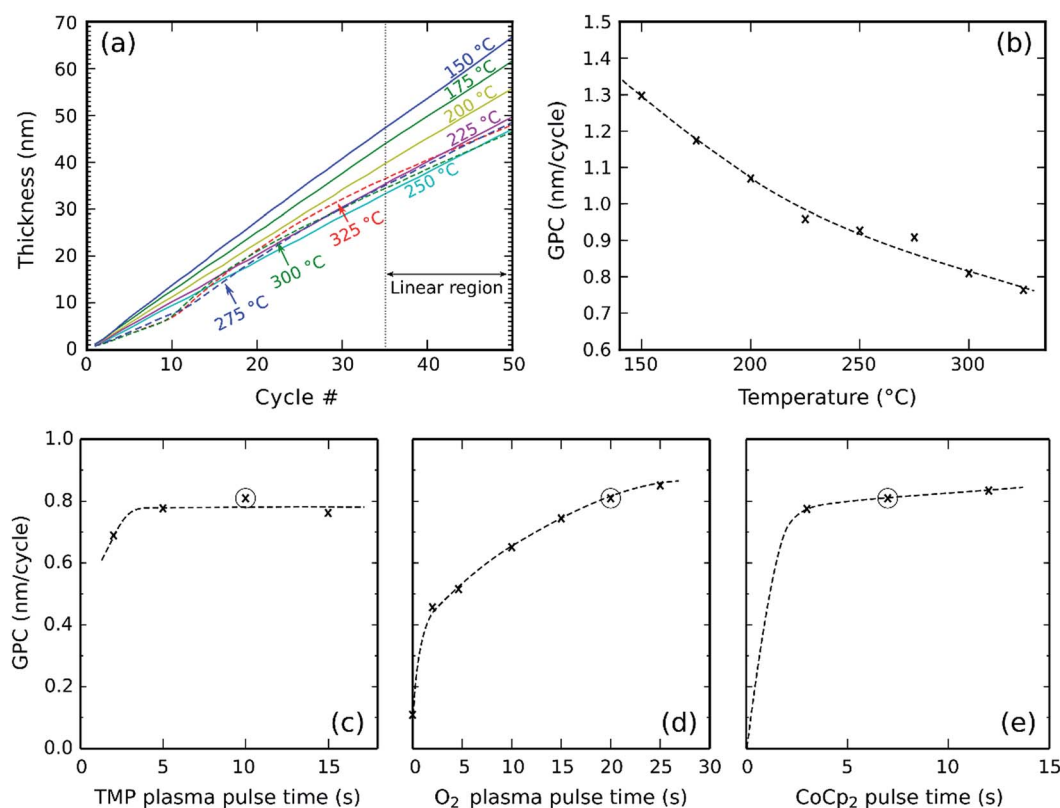

Fig. 1 Growth characterization of the cobalt phosphate process, showing (a) in situ growth curves between 150 and 325 °C; (b) the GPC as a function of the substrate temperature; and (c–e) the GPC as a function of the TMP plasma, O_2 plasma, and $CoCp_2$ pulse times, at 300 °C.

Phase characterization and conversion

The composition of the as-deposited cobalt phosphate was measured by ERD and RBS on a 100-cycle test sample deposited on a silicon substrate. The resulting depth profile is shown in Fig. 2. All elements are shown by their ERD traces, except for phosphorus, where the RBS trace is additionally plotted because it provides a better (lower-noise) signal. Because the depth information stems from atomic energy loss, which is proportional to the areal density (*i.e.* the product of the depth and the number density of atoms), the depth profile is primarily given as a function of the areal density (shown on the lower *x*-axis). To aid interpretation, an approximate depth scale in nm is shown on the secondary (upper) *x*-axis, based on linear scaling with the total film thickness.

The depth profile reveals a uniform film composition with an empirical stoichiometry of $CoP_{2.3}O_{6.7}$. Only a small amount of hydrogen (0.3%) was detected as an impurity. The composition is relatively phosphorus-rich and corresponds approximately to cobalt(IV) pyrophosphate, CoP_2O_7.

The phosphate starting materials were converted into phosphide catalysts either by thermal annealing or by electrochemical treatment. To produce the phosphide catalysts by thermal annealing, we employed the following synthesis route:

(1) Deposition of a metal phosphate ($M_xP_yO_z$, where M = Co,Fe) by PE-ALD.

(2) Conversion of the phosphate to a phosphide (M_xP, where M = Co,Fe) by post-deposition annealing in a reducing atmosphere.

This process was investigated in detail by *in situ* XRD during ramp annealing, as shown in Fig. 3. The test samples consisted of 100-cycle depositions of iron phosphate (Fig. 3a and b) and cobalt phosphate (Fig. 3c and d). Each sample was subjected to annealing in a reducing atmosphere consisting of 5% hydrogen in helium, while applying a linear temperature ramp from room temperature up to 950 °C at a rate of 5 °C min^{-1}. In both cases, the formation of crystalline phosphides could be clearly observed, starting from the corresponding as-deposited phosphates (which were amorphous,
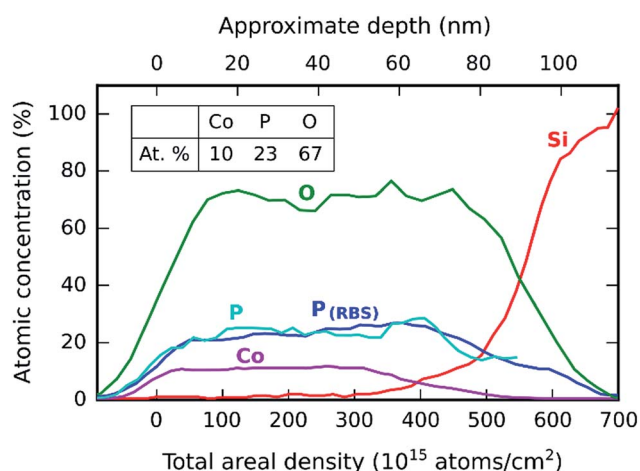

Fig. 2 Depth profile of a 100-cycle cobalt phosphate sample deposited on silicon and measured by ERD, with atomic percentages shown as a table inset.
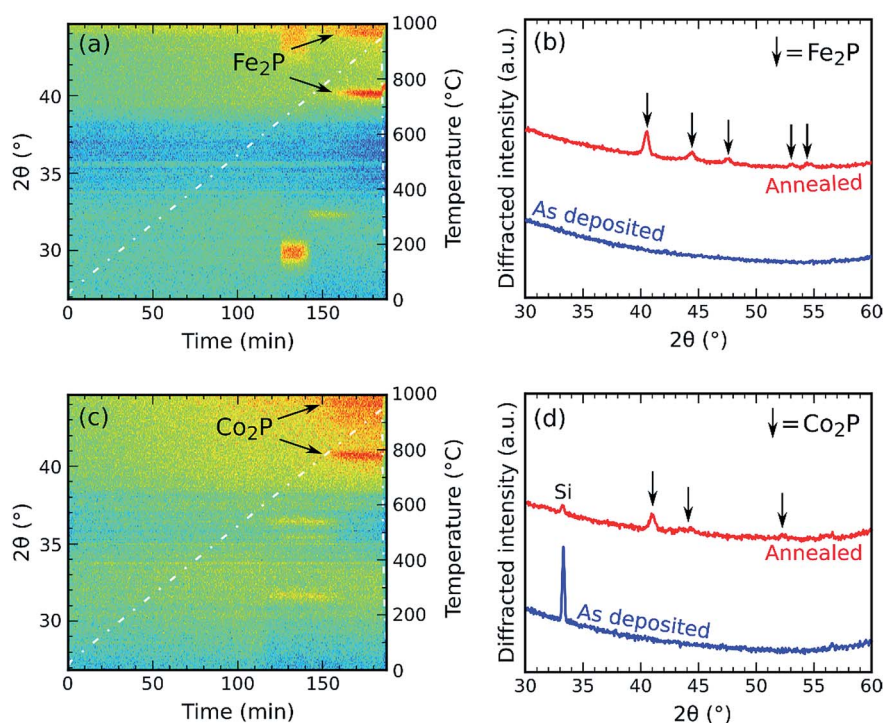

Fig. 3 Reduction of iron (a and b) and cobalt (c and d) phosphates to their respective phosphides by post-deposition annealing in a reducing atmosphere. Plots (a) and (c) show the evolution of the XRD intensity (color scale) together with temperature (white dashed line), while plots (b) and (d) show a comparison of the XRD patterns measured before and after annealing.

evidenced by the lack of initial diffraction peaks). More specifically, both Fe_2P (JCPDS #51-0943) and Co_2P (JCPDS #32-0306) were formed at a temperature of approx. 800 °C.

Aside from the fact that oxygen is removed, as is expected in a reduction reaction, it should be noted that the metal/phosphorus ratio of the produced phosphides differs considerably from the ratio of the starting materials, *i.e.* 2.0 for Co_2P and Fe_2P *versus* 0.43 for $CoP_{2.3}O_{6.7}$ and 0.67 for $FeP_{1.5}O_{4.7}$.[22] This means that excess phosphorus is either removed from the film, or remains embedded in an amorphous form (which would be invisible in XRD).

In order to find out which of those two possibilities holds, the cobalt phosphate/phosphide samples were analyzed by SEM/EDX, the results of which are shown in Fig. 4. The SEM images demonstrate the transformation from a smooth and featureless cobalt phosphate film (Fig. 4a) to a nanocrystalline cobalt phosphide film (Fig. 4b). The EDX spectra reveal that the amount of cobalt in the film remains unchanged during annealing, but both oxygen and phosphorus decrease dramatically in intensity. This leads to the conclusion that both oxygen and phosphorus are removed from the film during annealing, presumably through the following reduction reaction:

$$MP_zO_y + (3/2(z - x) + y) H_2 \rightarrow MP_x + (z - x) PH_3 \uparrow + y\, H_2O \uparrow$$
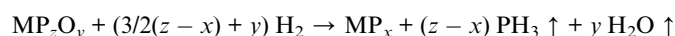
where M = Co,Fe, and $z > x$. In other words, the hydrogen in the reducing atmosphere removes oxygen from the film by converting it to water vapor and removes excess phosphorus by converting it to phosphine gas (PH_3). The result is a stoichiometric and crystalline metal phosphide. The production of phosphine gas, which is notorious for its toxicity and flammability, during this synthesis might lead to safety concerns. In this work, very thin films were processed and thus very low amounts of PH_3 could be produced. However, in case of performing this process on larger quantities of material, the release of PH_3 should be considered as a safety risk.

Electrocatalytic water oxidation

Fig. 5a shows the redox activity of as-deposited cobalt materials at pH 13 when exposed to positive potentials. As a reference to the cobalt-phosphate materials investigated in this work, a conventional cobalt oxide (Co_3O_4) was also deposited according to a known method.[25] The first redox wave (**1**) is assigned to an oxidation step from Co^{2+} to Co^{3+}, whereas the second wave (**2**) can be associated with the formation of a mixed Co^{3+}/Co^{4+} material, characteristic of cobalt oxyhydroxide water oxidation.[3,18,26,27] In the cobalt-oxide sample, the first redox wave is absent and the second wave is present to a much smaller extent, indicating the presence of a crystalline spinel phase with poor catalytic activity ($\eta_{10mA/cm^2} = 624$ mV), similar to that of ALD cobalt-oxide reported before.[18] The OER activity in this sample is caused by surface activity only, leading to higher overpotentials (Fig. 5b). This is supported by the much smaller specific capacitance measured for the cobalt-oxide sample (Fig. S2†). These data reconfirm the conclusions of other authors that Co_3O_4 with its crystalline spinel structure has lower activity compared to amorphous and layered (oxy)hydroxide materials, which have a much more flexible redox cycling behaviour.[3,18,26,27] The incorporation of phosphate by the newly developed ALD process endows the material with intrinsic disorder (Fig. 3d) and a propensity to form layered structures with phosphate anion interlayers. The flaky material structure observed by SEM and the non-stoichiometric incorporation of phosphate anions, indicated by XPS analysis, could point to the formation of such a layered double hydroxide (Fig. S3 and S4†). As a result, its catalytic OER activity is clearly enhanced ($\eta_{10mA/cm^2} = 509$ mV). This property may be exploited to develop biphasic catalytic-protective coatings in which a stable, crystalline underlayer is combined with a top layer of catalytically active material.[18] Despite the expected formation of hydroxide-containing material, phosphorus is retained within the structure, shown by post-OER XPS measurements (Fig. S4†). After extensive testing in alkaline medium, performance of the catalyst only slightly degraded and was still well above that of the cobalt oxide reference sample (Fig. S5†).

Electrocatalytic hydrogen evolution

The phosphate materials could be used for hydrogen evolution as well after an electrochemical activation procedure in alkaline conditions. Fig. 6 shows the very first cyclic voltammograms of as-deposited phosphate ALD materials in 0.1 M KOH. The cobalt-phosphate sample is characterised by a whimbrel-shaped first scan with cathodic currents. However, after initial reduction, the cobalt film is not reoxidized except for a small oxidation event at the end of the first scan.[9] Nonetheless, reorganization of the film and/or a slow reduction process does
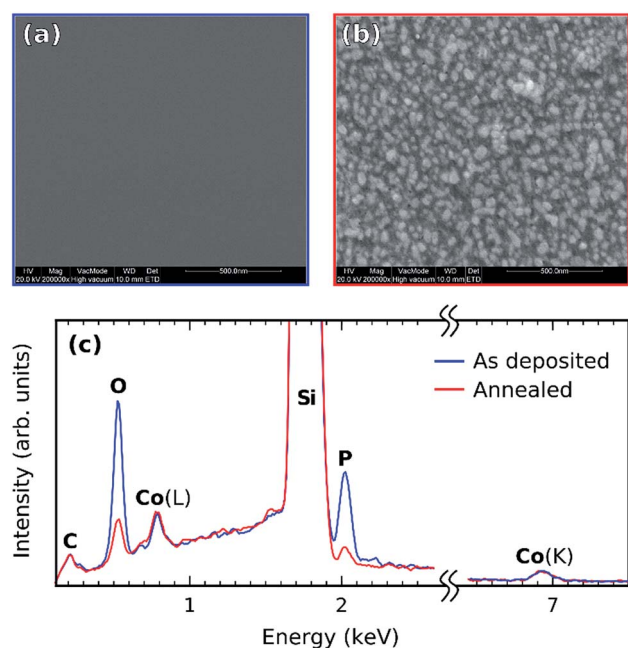

Fig. 4 SEM images showing the morphology of cobalt phosphate, (a) as-deposited and (b) after annealing in a reducing atmosphere, together with (c) a comparison between the EDX spectra of the same samples.
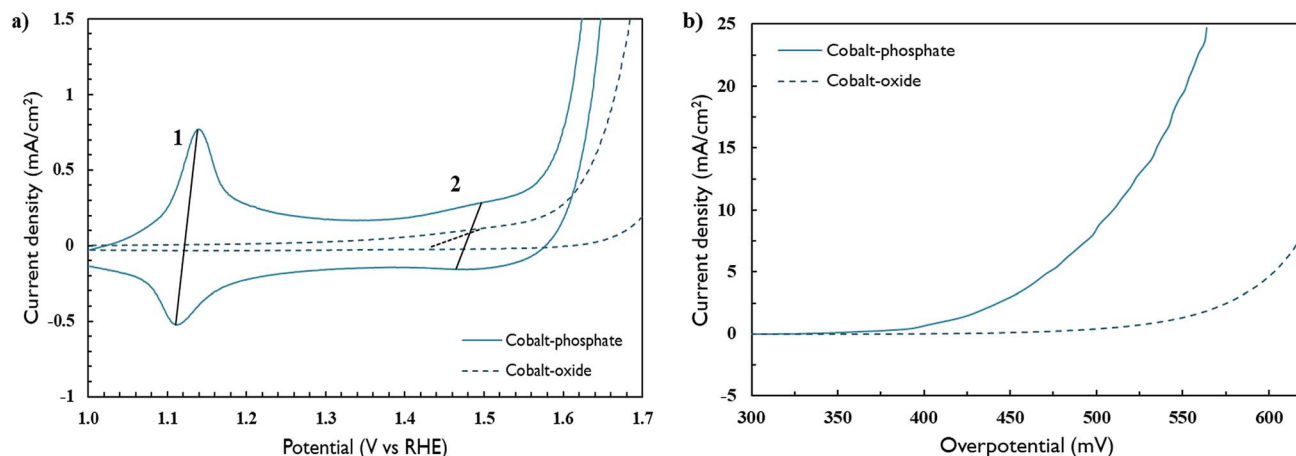
Fig. 5 Cyclic voltammetry of ALD as-deposited cobalt materials in 0.1 M KOH. (a) Close-up of pre-catalytic redox waves, obtained at a scan rate of 100 mV s^{-1}. (b) Steady-state catalytic oxidation current densities, obtained at a scan rate of 1 mV s^{-1}.

seem to continue over consecutive scans, as these result in a strong improvement of the performance. After prolonged cathodic current flow during the staircase voltammetry at low scan rate, the film reached its maximal performance. This activation procedure is accompanied with a ten-fold increase in film capacitance, indicating an increase in specific surface area (Fig. S6†). The first scan of iron-phosphate (Fig. 6b) is similar to that of cobalt-phosphate, but with much more pronounced cathodic current. Around −0.1 V *vs.* RHE, the iron-phosphate film displays multiple reversible redox events. Compared to the cobalt-phosphate film, performance quickly improves over consecutive scans and also reaches its maximal performance during staircase voltammetry.

Some samples first underwent a thermal treatment under a reducing H$_2$/He gas flow and were converted into Co$_2$P or Fe$_2$P (Fig. 3). For those materials, potential scanning did not result in any further improvement of the catalytic activity. Instead, optimal performance was already obtained from the first measurement (Fig. 7).

The activity of the electrochemically activated and thermally reduced materials in alkaline conditions is given in Fig. 7a. Cobalt oxide lacking phosphorus was also tested as a reference. The data show that the iron-based materials outperform cobalt-based materials, which is in accordance with literature.[6,8,12] However, iron-based materials appeared to be less stable than cobalt-containing materials (Fig. S7†). The thermally reduced materials, which were identified as having M$_2$P (M = Co,Fe) stoichiometry, are active both under alkaline and acidic (Fig. 7b and S7†) conditions. After reaction in alkaline conditions, reduced phosphide species are no longer present (Fig. S8†). This was also reported by Zhang *et al.* for Co$_2$P materials prepared by thermal phosphidation of ALD-deposited cobalt oxide films.[28] The cobalt oxide reference material was also active towards HER but had the lowest activity of all samples. After HER, the oxidation state of Co centers was clearly reduced with some metallic Co present (Fig. S10†). The electrochemically activated materials are superior to the thermally reduced. However, the electrochemically activated materials show no
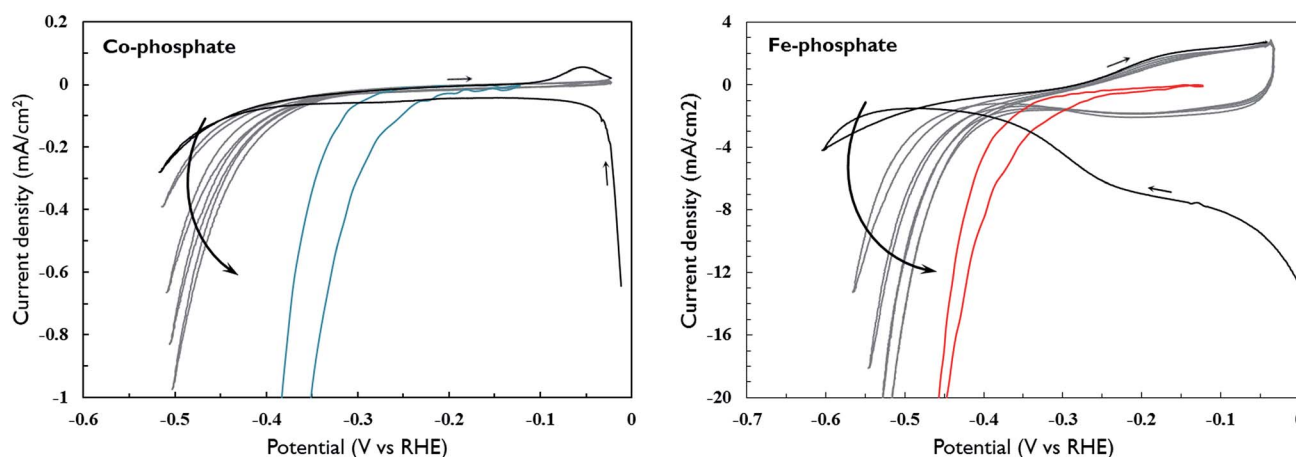

Fig. 6 Cyclic voltammetry of ALD as-deposited cobalt (left) and iron (right) phosphate materials in 0.1 M KOH. The very first (black) and subsequent (grey) scans were measured at a scan rate of 100 mV s^{-1}. Next, staircase cyclic voltammetry (coloured) was performed at 1 mV s^{-1}.
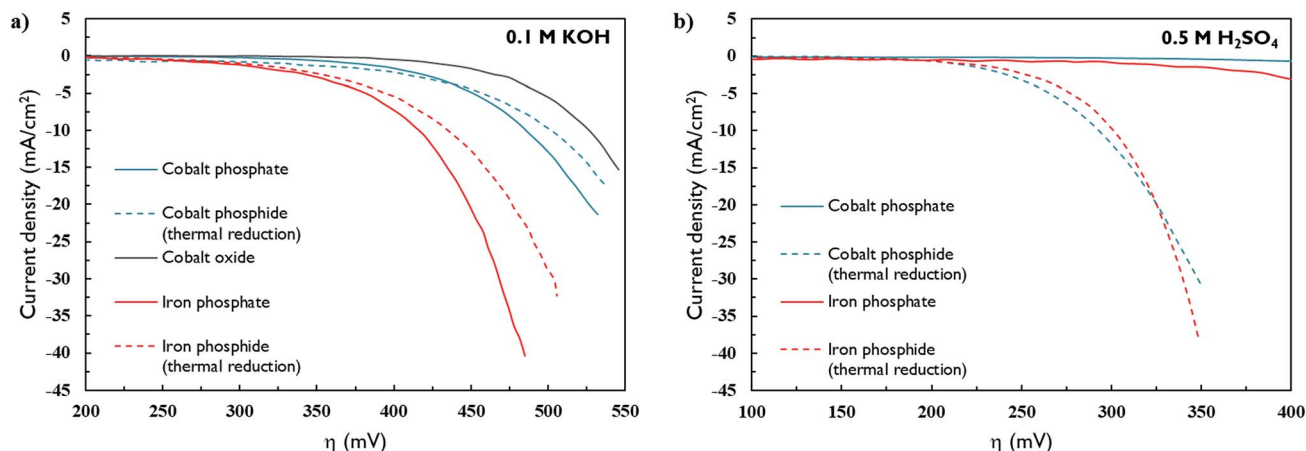
Fig. 7 Steady-state catalytic reduction current densities for electrochemically activated (full lines) or thermally annealed (dashed lines) cobalt and iron materials, obtained at a scan rate of 1 mV s^{-1} in (a) 0.1 M KOH and (b) 0.5 M H$_2$SO$_4$.

activity in acid medium. Following exposure to acid medium, their catalytic activity was lost in alkaline conditions as well, indicating dissolution of the film in acid medium. From this we infer that the electrochemically activated materials were not converted to pure M$_x$P phosphides. Others obtained materials with a phosphide/hydroxide surface layer when synthesizing metal-phosphide catalysts by electrochemical methods.[5,9,10] Such materials readily dissolve in acid media when not continuously exposed to sufficiently negative potentials.[5,9] XPS data identifies the material as a cobalt-phosphate with cobalt in a low oxidation state (Fig. S8†). SEM indicates a change in morphology from large crystallites to a thin film upon activation in alkaline medium (Fig. S11†).

For all materials, the required overpotential is quite high (η_{10mA/cm^2} = 416–502 mV (alkaline) and 293–301 mV (acid)). This can be explained by the low mass loadings in ALD films. When the results are plotted as a turnover frequency (TOF), the ALD films reported here show similar performance to other metal phosphide materials in acid medium (Fig. S12†). The turnover frequency is among the highest reported until now. This can be understood as follows. At very low mass loadings, every catalytic site operates at very high performance because mass transfer limitations are absent. This effect is enhanced in films that are prepared by ALD, because of its ability to obtain conformal coatings on irregular substrates.

Conclusions

Iron and cobalt phosphate materials were deposited by ALD and tested for water splitting activity. As-deposited cobalt phosphate was active towards oxygen evolution with clearly enhanced activity compared to a cobalt oxide sample lacking phosphate. Cobalt phosphate and iron phosphate were both active towards HER in alkaline medium. Initially, transient behaviour was observed while the metal atoms were being reduced to lower oxidation states. The resulting material was a metal (hydr)oxide containing phosphate species. Thermal reduction of the as-deposited metal phosphates resulted in the formation of

a metal phosphide (M$_2$P). In alkaline medium, these metal phosphides reconverted into phosphate-containing materials and were outperformed by the electrochemically reduced materials. In acid medium, only the thermally reduced phosphides were stable and active, achieving a performance that is similar to the state of the art.

In conclusion, we show that ALD is a valuable technique for depositing both oxide and phosphate materials directly onto surfaces. A post-deposition phosphidation step is not needed with the process demonstrated in this work. In alkaline medium, a bifunctional catalyst can be achieved even without the need for a thermal post-treatment. The films were active towards HER and OER, and their performance was comparable to the state of the art. More research is desirable to uncover the nature of the active sites as obtained by different deposition methods.

Conflicts of interest

There are no conflicts to declare.

Acknowledgements

References

1 M. W. Kanan and D. G. Nocera, In Situ Formation of an Water Containing Phosphate and Co^{2+}, *Science*, 2008, **321**, 1072–1075.
2 Y. Surendranath, D. a Lutterman, Y. Liu and D. G. Nocera, Nucleation, growth, and repair of a cobalt-based oxygen evolving catalyst, *J. Am. Chem. Soc.*, 2012, **134**, 6326–6336.

3 J. B. Gerken, *et al.*, Electrochemical water oxidation with cobalt-based electrocatalysts from pH 0–14: the thermodynamic basis for catalyst structure, stability, and activity, *J. Am. Chem. Soc.*, 2011, **133**, 14431–14442.

4 L. G. Bloor, P. I. Molina, M. D. Symes and L. Cronin, Low pH electrolytic water splitting using earth-abundant metastable catalysts that self-assemble in situ, *J. Am. Chem. Soc.*, 2014, **136**, 3304–3311.

5 S. Cobo, *et al.*, A Janus cobalt-based catalytic material for electro-splitting of water, *Nat. Mater.*, 2012, **11**, 802–807.

6 E. J. Popczun, C. G. Read, C. W. Roske, N. S. Lewis and R. E. Schaak, Highly active electrocatalysis of the hydrogen evolution reaction by cobalt phosphide nanoparticles, *Angew. Chem., Int. Ed.*, 2014, **53**, 5427–5430.

7 I. Roger, M. A. Shipman and M. D. Symes, Earth-abundant catalysts for electrochemical and photoelectrochemical water splitting, *Nat. Rev. Chem.*, 2017, **1**, 3.

8 J. F. Callejas, C. G. Read, C. W. Roske, N. S. Lewis and R. E. Schaak, Synthesis, Characterization, and Properties of Metal Phosphide Catalysts for the Hydrogen-Evolution Reaction, *Chem. Mater.*, 2016, **28**, 6017–6044.

9 F. H. Saadi, *et al.*, CoP as an acid-stable active electrocatalyst for the hydrogen-evolution reaction: electrochemical synthesis, interfacial characterization and performance evaluation, *J. Phys. Chem. C*, 2014, **118**, 29294–29300.

10 N. Jiang, B. You, M. Sheng and Y. Sun, Electrodeposited Cobalt-Phosphorous-Derived Films as Competent Bifunctional Catalysts for Overall Water Splitting, *Angew. Chem., Int. Ed.*, 2015, **54**, 6251–6254.

11 A. Dutta and N. Pradhan, Developments of Metal Phosphides as Efficient OER Precatalysts, *J. Phys. Chem. Lett.*, 2017, **8**, 144–152.

12 J. F. Callejas, *et al.*, Electrocatalytic and photocatalytic hydrogen production from acidic and neutral-pH aqueous solutions using iron phosphide nanoparticles, *ACS Nano*, 2014, **8**, 11101–11107.

13 P. Jiang, *et al.*, A Cost-Effective 3D Hydrogen Evolution Cathode with High Catalytic Activity: FeP Nanowire Array as the Active Phase, *Angew. Chem., Int. Ed.*, 2014, **53**, 12855–12859.

14 Y. Yan, *et al.*, A Flexible Electrode Based on Iron Phosphide Nanotubes for Overall Water Splitting, *Chem.–Eur. J.*, 2015, **21**, 18062–18067.

15 J. Kibsgaard, *et al.*, Designing an improved transition metal phosphide catalyst for hydrogen evolution using experimental and theoretical trends, *Energy Environ. Sci.*, 2015, **8**, 3022–3029.

16 R. Liu, Z. Zheng, J. Spurgeon and X. Yang, Enhanced photoelectrochemical water-splitting performance of semiconductors by surface passivation layers, *Energy Environ. Sci.*, 2014, **7**, 2504–2517.

17 F. Mattelaer, *et al.*, Manganese oxide films with controlled oxidation a combination of atomic layer deposition and post-deposition annealing, *RSC Adv.*, 2016, **6**, 98337–98343.

18 J. Yang, J. K. Cooper, F. M. Toma, K. A. Walczak, M. Favaro, J. W. Beeman, L. H. Hess, C. Wang, C. Zhu, S. Gul, J. Yano, C. Kisielowski, A. Schwartzberg and I. D. Sharp, A multi-functional biphasic water splitting catalyst tailored for integration with high performance semiconductor photoanodes, *Nat. Mater.*, 2017, **16**, 335–341.

19 A. Goryachev, *et al.*, Stability of CoPx Electrocatalysts in Continuous and Interrupted Acidic Electrolysis of Water, *ChemElectroChem*, 2018, **5**, 1230–1239.

20 V. Di Palma, *et al.*, Atomic layer deposition of cobalt phosphate thin films for the oxygen evolution reaction, *Electrochem. Commun.*, 2019, **98**, 73–77.

21 K. B. Gandrud, A. Pettersen, O. Nilsen and H. Fjellvåg, High-performing iron phosphate for enhanced lithium ion solid state batteries as grown by atomic layer deposition, *J. Mater. Chem. A*, 2013, **1**, 9054–9059.

22 T. Dobbelaere, F. Mattelaer, J. Dendooven, P. Vereecken and C. Detavernier, Plasma-Enhanced Atomic Layer Deposition of Iron Phosphate as a Positive Electrode for 3D Lithium-Ion Microbatteries, *Chem. Mater.*, 2016, **28**, 3435–3445.

23 J. Liu, *et al.*, Atomic layer deposition of amorphous iron phosphates on carbon nanotubes as cathode materials for lithium-ion batteries, *Electrochim. Acta*, 2015, **162**, 275–281.

24 T. Dobbelaere, A. K. Roy, P. Vereecken and C. Detavernier, Atomic layer deposition of aluminum phosphate based on the plasma polymerization of trimethyl phosphate, *Chem. Mater.*, 2014, **26**, 6863–6871.

25 M. E. Donders, H. C. M. Knoops, M. C. M. van, W. M. M. Kessels and P. H. L. Notten, Remote Plasma Atomic Layer Deposition of Co_3O_4 Thin Films, *J. Electrochem. Soc.*, 2011, **158**, G92.

26 L. Trotochaud, J. K. Ranney, K. N. Williams and S. W. Boettcher, Solution-cast metal oxide thin film electrocatalysts for oxygen evolution, *J. Am. Chem. Soc.*, 2012, **134**, 17253–17261.

27 J. A. Koza, Z. He, A. S. Miller and J. A. Switzer, Electrodeposition of crystalline Co_3O_4-A catalyst for the oxygen evolution reaction, *Chem. Mater.*, 2012, **24**, 3567–3573.

28 Y. Zhang, L. Gao, E. J. M. Hensen and J. P. Hofmann, Evaluating the Stability of Co_2P Electrocatalysts in the Hydrogen Evolution Reaction for Both Acidic and Alkaline Electrolytes, *ACS Energy Lett.*, 2018, **3**, 1360–1365.